

## Self-Assembly

## Double-Gyroid Nanostructure Formation by Aggregation-Induced Atropisomerization and Co-Assembly of Ionic Liquid-Crystalline Amphiphiles

Nanami Uemura, Tsubasa Kobayashi, Shintaro Yoshida, Ya-xin Li, Karel Goossens, Xiangbing Zeng, Go Watanabe, and Takahiro Ichikawa\*

**Abstract:** We report a new molecular-design principle for creating double-gyroid nanostructured molecular assemblies based on atropisomerization. Ionic amphiphiles containing two imidazolium rings close to each other were designed and synthesized. NMR data revealed that the rotation of the imidazolium rings is restricted, with an activation energy as high as  $63 \text{ kJ mol}^{-1}$  in DMSO- $d_6$  solution (DFT prediction for a model compound in the vacuum:  $90\text{--}100 \text{ kJ mol}^{-1}$ ). Due to the restricted rotation, the amphiphiles feature “double” atropisomeric axes in their ionic segments and form three stable atropisomers: meso, R, and S. These isomers co-organize into  $Ia\bar{3}d$ -type bicontinuous cubic liquid-crystalline mesophases through nanosegregation of the ionic and non-ionic parts. Considering the intrinsic characteristic of  $Ia\bar{3}d$ -type bicontinuous cubic structures that they are composed of intertwined right- and left-handed single gyroids, we propose that the simultaneous presence of both R- and S-atropisomers is an important contributor to the formation of double-gyroid structures.

Double-gyroid structures are a class of 3D periodic structures with an  $Ia\bar{3}d$  cubic symmetry.<sup>[1]</sup> They are composed of two interwoven networks of 3D branched channel structures. Owing to the unique structural characteristics, functional

How to cite: *Angew. Chem. Int. Ed.* **2020**, *59*, 8445–8450  
International Edition: doi.org/10.1002/anie.202000424  
German Edition: doi.org/10.1002/ange.202000424

materials forming such bicontinuous cubic ( $\text{Cub}_{\text{bi}}$ ) structures have been actively pursued to achieve, for example, efficient mass transport,<sup>[2]</sup> drug delivery,<sup>[3]</sup> or catalysis.<sup>[4]</sup> Several liquid-crystalline (LC) molecules that adopt thermotropic  $\text{Cub}_{\text{bi}}$  mesophases have been shown to self-organize into double-gyroid nanostructures.<sup>[5]</sup> This class of nanostructured materials has attracted increasing attention because of their potential utility as “alignment-free” nanochanneled materials for size-selective separation membranes<sup>[6]</sup> or conductive matrices.<sup>[7]</sup>

Out of tens of thousands of reported LC molecules, relatively few exhibit  $\text{Cub}_{\text{bi}}$  phases.<sup>[5,8]</sup> The molecular requirements to achieve such mesophases are not yet fully understood, although there is a small degree of understanding on the characteristics of the molecular structures forming  $\text{Cub}_{\text{bi}}$  phases.<sup>[5–10]</sup> Because of the technological potential as nanochannel materials, it is important to establish molecular-design principles for obtaining  $\text{Cub}_{\text{bi}}$  liquid crystals. One significant clue is the fact that double-gyroid structures are composed of two screw helices of opposite handedness which are mirror images of each other.

Previous studies on thermotropic  $\text{Cub}_{\text{bi}}$  liquid crystals have identified roughly three mechanisms that may lead to  $Ia\bar{3}d$ -type  $\text{Cub}_{\text{bi}}$  mesophases (Figure 1). In case I, achiral rod- or disc-shaped LC molecules incidentally form, through nucleation, a left- or right-handed helical assembly in one domain and a helix of opposite handedness in a neighboring domain to optimize space-filling.<sup>[5b,11]</sup> Case II has been found for racemic mixtures of chiral LC molecules.<sup>[12]</sup> When such mixtures form supramolecular assemblies, there is a possibility that, locally, the ratio of R- and S-isomers slightly deviates from 1:1. Such deviations result in the formation of both right- and left-handed domains and the creation of double gyroid structures. Case III was reported by Tschierske and co-workers for polycatenar rod-like molecules based on a 5,5'-diphenylbithiophene core.<sup>[13]</sup> These achiral compounds locally form right- or left-handed chiral assemblies as a result of chirality synchronization of the close-packed molecules. In this case, the enantiomerization has an activation energy of only  $2.7 \text{ kJ mol}^{-1}$ . In all three cases, the LC molecules form twisted assemblies to reduce packing frustrations, and the supramolecular assemblies further organize into double-gyroid structures.


Considering the importance of right- and left-handed helix formation for inducing  $\text{Cub}_{\text{bi}}$  phases, we decided to focus on molecular building blocks that form atropisomers, that is, stereoisomers that may occur when free rotation about


[\*] N. Uemura, T. Kobayashi, T. Ichikawa  
Department of Biotechnology  
Tokyo University of Agriculture and Technology  
Tokyo 184-8588 (Japan)  
E-mail: t-ichi@cc.tuat.ac.jp

S. Yoshida, G. Watanabe  
Department of Physics, School of Science, Kitasato University  
Sagamihara, Kanagawa 252-0373 (Japan)

Y. Li, X. Zeng  
Department of Materials Science and Engineering  
University of Sheffield  
Sheffield, S1 3JD (UK)

K. Goossens  
Center for Multidimensional Carbon Materials (CMCM)  
Institute for Basic Science (IBS)  
Ulsan 44919 (Republic of Korea)

 The ORCID identification number(s) for the author(s) of this article can be found under: <https://doi.org/10.1002/anie.202000424>.

 © 2020 The Authors. Published by Wiley-VCH Verlag GmbH & Co. KGaA. This is an open access article under the terms of the Creative Commons Attribution License, which permits use, distribution and reproduction in any medium, provided the original work is properly cited.

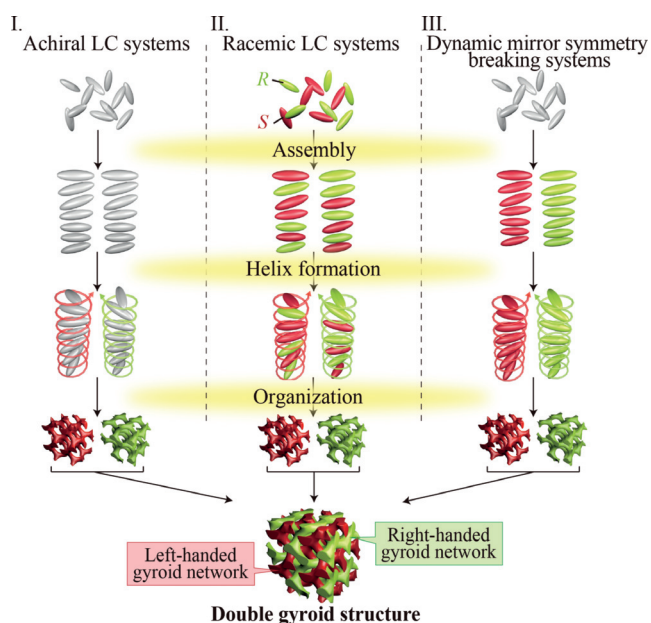


**Figure 1.** Schematic illustration of the different formation mechanisms for thermotropic  $la\bar{3}d$   $Cub_{Bi}$  mesophases. Two helical nanostructures of opposite handedness co-organize into double gyroid structures. Case I: Achiral molecules form neighboring right-handed and left-handed helix domains. Case II: Racemic mixtures of chiral molecules form two helix domains of opposite handedness. Case III: Dynamic mirror-symmetry breaking of achiral molecules spontaneously produces right- and left-handed helices.

a particular bond is prohibited by, for example, steric hindrance.<sup>[14]</sup> Atropisomers have been intensively explored for designing asymmetric catalysts.<sup>[15]</sup> More recently, there have been several reports of organic compounds that form atropisomers only in aggregated states.<sup>[16]</sup> One of the key factors that play a role in this phenomenon is the restriction of intramolecular rotation upon close-packing of the molecules. We envisioned that exploitation of such aggregation-induced atropisomerization (AIA) could be a new way of designing  $Cub_{Bi}$  liquid crystals. The polycatenar rod-like LCs that were reported by Tschierske and co-workers<sup>[13]</sup> can be considered to be the first examples of  $Cub_{Bi}$  liquid crystals based on AIA phenomena.

In the present study, the molecular design was inspired by work of Claramunt et al., who synthesized benzene derivatives containing two 2-methyl-1-imidazolyl groups.<sup>[17]</sup> They reported that, for the *ortho*-disubstituted derivatives, rotation about the C–N bonds between the benzene ring and the two imidazole rings ( $C_{benzene}-N$ ) is sterically hindered, giving rise to the formation of atropisomers. We modified the original structures of Claramunt et al. and designed a 1,2-dicyanobenzene having two 2-methyl-1-imidazolyl moieties in the 4- and 5-positions (DCB- $Im_2$ , Figure 2a). To estimate the energy barrier for rotation of the imidazole rings, DFT calculations were performed for DCB- $Im_2$  in vacuum. After defining the dihedral angles  $\phi$  and  $\psi$  as shown in Figure 2b, we estimated the energy barriers for rotation about the  $C_{benzene}-N$  bonds and constructed a 2D potential-energy map (Figure 2c). The map revealed four zones (I, I', II, and III; indicated in blue)

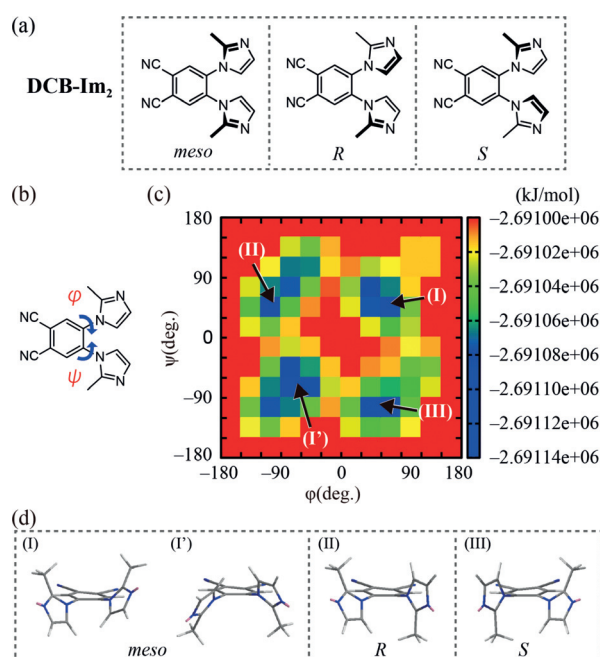


**Figure 2.** a) Molecular structure of DCB- $Im_2$ . The molecule can adopt three stable conformations: *meso*, *R*, and *S*. b) Definition of dihedral angles  $\phi$  and  $\psi$ . c), d) 2D potential energy map showing the energy barriers for rotation about the  $C_{benzene}-N$  bonds (dihedral angles  $\phi$  and  $\psi$ ) in DCB- $Im_2$ , as obtained from DFT calculations. Four stable conformer regions were identified and designated as I/I', II, and III, corresponding to the *meso*, *R*, and *S* conformers, respectively.

corresponding to stable conformers in which the two imidazole rings are tilted by circa  $30^\circ$  relative to the plane of the dicyanobenzene ring to form either “parallel” (*meso*) or “antiparallel” (*R* or *S*) isomers (Figure 2d).<sup>[18]</sup> It is noteworthy that the energy barriers that separate the four blue regions in Figure 2c are about  $90\text{--}100\text{ kJ mol}^{-1}$ . Considering previous insights into the relationship between the rotation energy barrier and atropisomer formation,<sup>[19]</sup> an energy barrier of circa  $100\text{ kJ mol}^{-1}$  seems to be sufficient for inducing permanent atropisomers even in solution. It can be expected that a slightly smaller energy barrier is already effective for suppressing the interconversion of isomers in bulk aggregation states.

Following twofold quaternization, the DCB- $Im_2$  fragment was used as the ionic headgroup of amphiphilic block molecules ( $1_n-X$ , Figure 3;  $n$ : number of carbon atoms in the alkyl chains, X: anion species) for which we examined the relationships between atropisomerization and self-organization.

To experimentally confirm the occurrence of atropisomerism for the ionic headgroup of  $1_n-X$ , a solution of compound  $1_{14}$ -TFSI in DMSO- $d_6$  was subjected to  $^1H$  NMR measurements at room temperature. Signals of the protons at the 4- and 5-positions of the imidazolium rings (that is,  $H_4$  and  $H_5$ ) were observed as broad, overlapping peaks in the range  $7.40\text{--}8.00\text{ ppm}$ . Through deconvolution of the overlapping peaks by Lorentzian peak-fitting, we found that there were three peaks, a ( $7.75\text{ ppm}$ ), b ( $7.66\text{ ppm}$ ), and c ( $7.56\text{ ppm}$ ) with a peak-area ratio of about  $3:5:2$ . To identify the three peaks,

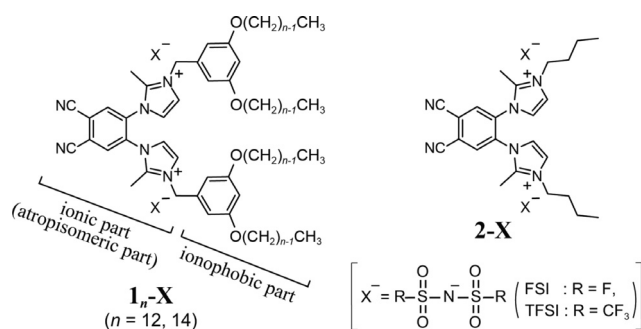


**Figure 3.** Molecular structures of ionic amphiphilic molecules  $1_n\text{-X}$  and model compounds  $2\text{-X}$ .

a NOESY experiment, which is a 2D NMR method to yield through-space correlations via spin-lattice relaxation, was performed. The obtained profile is shown in Figure 4. It should be noted that the proton signals of the methylene groups in the benzyl groups appear at 5.33 ppm (peak f) and those of the benzene rings appear at 6.34 and 6.46 ppm (peaks e and d), respectively. Since compound  $1_{14}\text{-TFSI}$  has two imidazolium rings, we define them as  $\text{Im}_1$  and  $\text{Im}_2$  as shown in Figure 4a in order to make discussion clear. It is notable that peak b shows cross-peaks with peak e and f. Taking into account the results of previous studies on NOESY experiments for imidazolium compounds,<sup>[20]</sup> peak b could be assigned to  $\text{H}_4$ , which is close to the benzyl group. Consequently, peak a and c can be assigned to  $\text{H}_5$  with consideration of the peak-area ratio of the three peaks. Focusing on peak a and c, it can be seen that peak a shows weak correlations with peak e and f while peak c shows no correlation. Based on the previous studies referred to

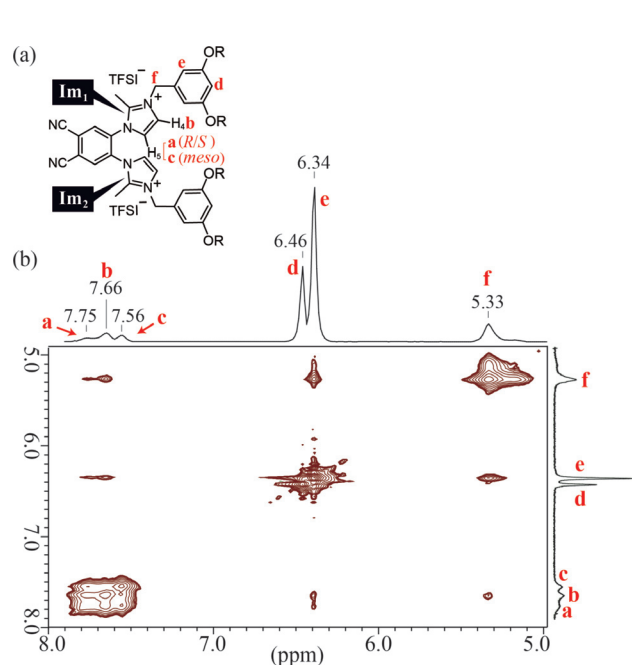


**Figure 4.** a) Molecular structure of  $1_{14}\text{-TFSI}$ . The two imidazolium rings are defined as  $\text{Im}_1$  and  $\text{Im}_2$ . b)  $^1\text{H}$  NOESY NMR profile of  $1_{14}\text{-TFSI}$  in  $\text{DMSO-}d_6$ , recorded on a 400 MHz spectrometer at 23 °C.

above,<sup>[20]</sup> it becomes evident that the proton at 5-position of the imidazolium ring shows no cross-peak with the proton of the methylene groups at the 3-position of the imidazolium ring. These insights lead us to conclude that the weak cross-peak between peaks a and e, f are attributed to the correlation between  $\text{H}_5$  of  $\text{Im}_1$  and the protons of the benzyl group from the other imidazolium ring  $\text{Im}_2$ . Since it is expected that  $\text{H}_5$  of  $\text{Im}_1$  gets closer to the methylene group of  $\text{Im}_2$  in the *R/S* conformers than in the *meso* conformer, peak a can be assigned to  $\text{H}_5$  in the *R/S* conformers while peak c can be assigned to the same proton in the *meso* conformer.

With the aim to examine the temperature dependence of the atropisomerism,  $^1\text{H}$  NMR measurements were performed for a solution of compound  $1_{14}\text{-TFSI}$  in  $\text{DMSO-}d_6$  at various temperatures (Figure 5). As mentioned above,  $\text{H}_4$  appears as a broad peak at 7.70 ppm (peak b) whereas  $\text{H}_5$  appears as two broad signals centered at slightly different ppm values depending on the type of conformer: 7.79 ppm for *R/S*-conformers (peak a) and 7.60 ppm for *meso* conformers (peak c) at 30 °C. The peak-area ratio between a(*R/S*) and c(*meso*) was measured to be 13:12, reflecting the relative populations of the isomers. Upon heating the solution, the two signals corresponding to the *R/S* and *meso* conformers gradually coalesced to become a single peak centered at 7.65 ppm. The latter value is consistent with the weighted average position of a(*R/S*) and c(*meso*). The observed behavior can be explained by the increasingly fast interconversion of the conformers upon heating. Based on the variable-temperature  $^1\text{H}$  NMR data and using the Eyring equation,<sup>[19]</sup> the energy barrier for rotation about the  $\text{C}_{\text{benzene}}\text{-N}$  bonds was estimated to be 63  $\text{kJ mol}^{-1}$  (see the Supporting Information). Similar experiments were carried out for model compound  $2\text{-TFSI}$ . As for

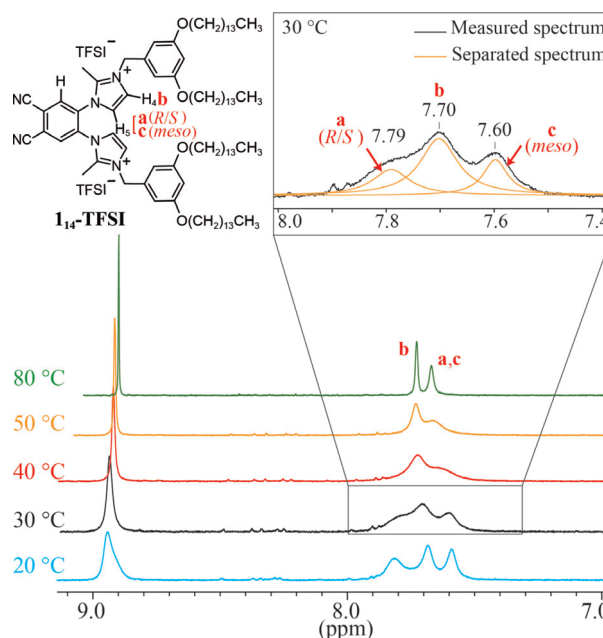


**Figure 5.**  $^1\text{H}$  NMR spectra of  $1_{14}\text{-TFSI}$  in  $\text{DMSO-}d_6$ , recorded on a 500 MHz spectrometer over a range of temperatures (20–80 °C). Deconvolution of peaks in the range 7.40–8.00 ppm was achieved by Lorentzian peak-fitting.



$\mathbf{1}_{14}$ -TFSI, the occurrence of *R/S* and *meso* isomers was observed for  $\mathbf{2}$ -TFSI, and the energy barrier for conformational interconversion was estimated to be  $64 \text{ kJ mol}^{-1}$  (see the Supporting Information, Figure S20). Although the aforementioned energy barriers are lower than the value of  $100 \text{ kJ mol}^{-1}$ , which is considered to be a prerequisite for the permanent existence of different atropisomers, the results strongly suggest that, in solution, the rotation about the  $\text{C}_{\text{benzene}}-\text{N}$  bonds is hindered to some extent. It can be expected that in bulk LC states, the rotation is even more restricted, giving rise to AIA phenomena. Further details about the NMR experiments can be found in the Supporting Information (Figures S21–S25).

Next, the thermal phase behaviors of salts  $\mathbf{1}_n\text{-X}$  in the bulk were examined using polarized-light optical microscopy (POM), differential scanning calorimetry (DSC), and X-ray diffraction measurements. Compounds  $\mathbf{1}_n\text{-X}$  show thermotropic  $\text{Cub}_{\text{bi}}$  and hexagonal-columnar ( $\text{Col}_{\text{h}}$ ) phases as a result of nanosegregation of the ionic moieties and the flexible, ionophobic molecular segments. The phase-transition temperatures are summarized in Figure 6a.  $\text{Cub}_{\text{bi}}$  phases were observed for  $\mathbf{1}_{14}$ -FSI and  $\mathbf{1}_{14}$ -TFSI. For example, upon cooling a sample of  $\mathbf{1}_{14}$ -TFSI from its isotropic liquid (Iso) state, a focal conic texture appeared at  $127^\circ\text{C}$  (Figure 6b, left). Upon further cooling, the POM texture started to disappear at around  $78^\circ\text{C}$ , indicating the transition to an optically isotropic  $\text{Cub}_{\text{bi}}$  phase (Figure 6b, center and right).

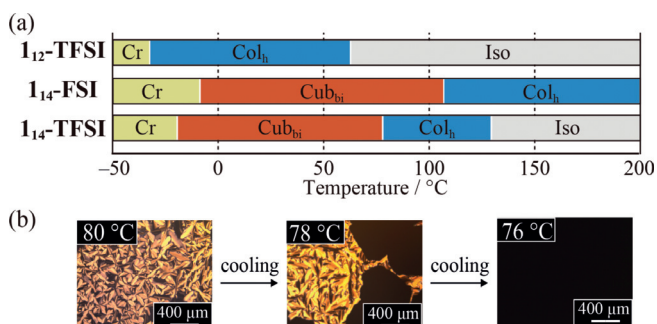


**Figure 6.** a) Thermotropic LC properties of  $\mathbf{1}_n\text{-X}$  upon cooling. Cr, crystalline;  $\text{Col}_{\text{h}}$ , hexagonal columnar;  $\text{Cub}_{\text{bi}}$ , bicontinuous cubic; Iso, isotropic. c) Polarized-light optical microscopy images of  $\mathbf{1}_{14}$ -TFSI, showing the phase transition from the  $\text{Col}_{\text{h}}$  to  $\text{Cub}_{\text{bi}}$  phase.

Synchrotron-based small-angle X-ray scattering (SAXS) measurements were performed to obtain further insight into the LC mesophases adopted by compounds  $\mathbf{1}_{14}$ -FSI and  $\mathbf{1}_{14}$ -TFSI. Figure 7a shows SAXS patterns of  $\mathbf{1}_{14}$ -FSI that were recorded at various temperatures during heating. The SAXS pattern recorded at  $170^\circ\text{C}$  shows one intense peak and four weak peaks, which were indexed as the (10), (11), (20), (21), and (30) reflections of a 2D hexagonal arrangement of columns (hence,  $\text{Col}_{\text{h}}$ ) with a lattice parameter  $a$  of  $40.6 \text{ \AA}$ . The SAXS pattern recorded at  $120^\circ\text{C}$  shows two intense peaks and thirteen weak peaks, which were indexed as the (211), (220), (321), (400), (420), (332), (422), (521), (440), (611)/(532), (541), (631), (444), (543), and (633) reflections of a 3D cubic structure with  $Ia\bar{3}d$  symmetry and a lattice

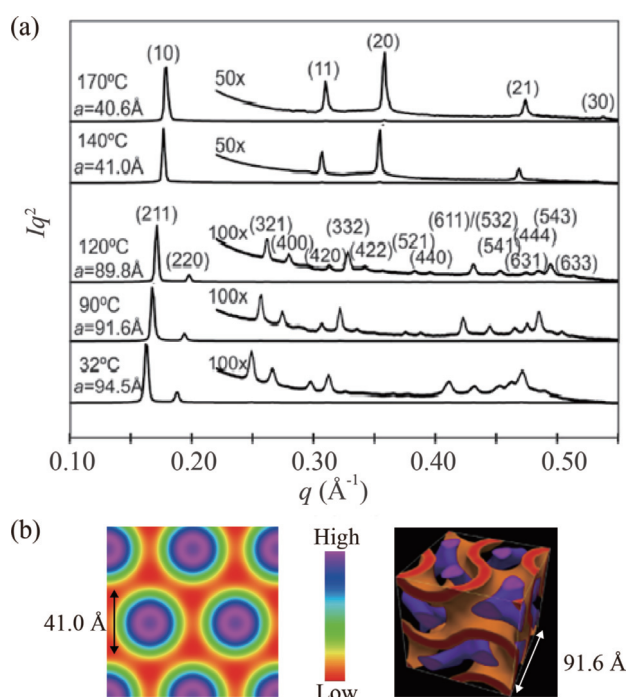


**Figure 7.** a) Small-angle X-ray scattering patterns of  $\mathbf{1}_{14}$ -FSI, recorded at various temperatures during heating. b) Reconstructed electron density maps of the  $\text{Col}_{\text{h}}$  phase of  $\mathbf{1}_{14}$ -FSI at  $140^\circ\text{C}$  (2D map) and of the  $Ia\bar{3}d\text{-Cub}_{\text{bi}}$  phase of  $\mathbf{1}_{14}$ -FSI at  $90^\circ\text{C}$  (3D map).

parameter  $a$  of  $89.8 \text{ \AA}$ . Further details are provided in the Supporting Information (Figures S17–S19). Based on the experimental SAXS intensities for the  $\text{Col}_{\text{h}}$  and  $\text{Cub}_{\text{bi}}$  phases, electron-density maps were reconstructed (Figure 7b). The high- and low-electron-density regions are colored in purple and red, respectively. The high-density regions appear in the center of the nanochannels in the  $\text{Col}_{\text{h}}$  and  $\text{Cub}_{\text{bi}}$  phases. These results are consistent with a localization of the ionic parts of  $\mathbf{1}_n\text{-X}$  in the interior of the nanochannels, as was previously found for wedge-shaped ionic liquid crystals forming  $\text{Col}_{\text{h}}$  and  $\text{Cub}_{\text{bi}}$  phases.<sup>[2b,7a]</sup>

Based on the SAXS data and considering the molecular structures and volumes of compounds  $\mathbf{1}_n\text{-X}$ , the organization into  $\text{Col}_{\text{h}}$  and  $\text{Cub}_{\text{bi}}$  mesophases occurs via self-assembly of about three molecules into supramolecular discs that stack on top of each other (see Figure S26). As mentioned above, the NMR results in solution indicated that rotation about the  $\text{C}_{\text{benzene}}-\text{N}_{\text{imidazolium}}$  bonds is restricted to some extent. The hindrance of free rotation is expected to significantly increase upon aggregation, thus endowing  $\mathbf{1}_n\text{-X}$  with quasi-permanent chirality as a result of AIA. We hypothesize that, upon formation of the bulk LC mesophases, packing frustrations are slightly reduced by locally enantiopure stacking of the *R*- and *S*-enantiomers, respectively. Hence, the ratio of *R*- and *S*-isomers may locally deviate from 1:1 (as shown in Figure 1, case II), leading to the creation of double-gyroid structures. It should be noted that it is impossible to exclude the possibility that the present LC system proceeds via case III if  $\mathbf{1}_n\text{-X}$  molecules have an ability to change the conformation of other neighboring molecules, as is the case for the LC systems reported by Tschierske.<sup>[13]</sup> It should also be noted that there

are many double-gyroid structures of non-chiral compounds, such as block copolymers and dendrimers,<sup>[1c,2a,21]</sup> which means that helical molecular assemblies or chiral molecular structures are not essential for the formation of double-gyroid structures. For inducing the formation of double-gyroid structures in the case of these materials, it is generally understood that the volume balance between the mutually incompatible blocks is known to be a key factor. This idea is also true in the case of LC block molecules. Considering a fact that only a limited number of ionic liquid crystals have been reported to exhibit thermotropic  $Cub_{bi}$  phases although a variety of ionic LC compounds have been designed,<sup>[2b,7,22,23]</sup> we believe that the emergence of double-gyroid  $Ia\bar{3}d$  cubic phases for  $\mathbf{1}_{14}$ -X is also partially promoted by their organization into twisted assemblies as well as the effects of the volume balance between the ionic/non-ionic parts.

In summary, we have designed novel ionic block molecules  $\mathbf{1}_n$ -X that may adopt three stable conformations. NMR-spectroscopic measurements revealed a significant energy barrier of  $\approx 63$  kJ mol<sup>-1</sup> in DMSO-*d*<sub>6</sub> solution for the inter-conversion between the stable conformers of  $\mathbf{1}_n$ -X through rotation about the C–N bonds linking the benzene and imidazolium rings. The high experimentally obtained energy barrier was consistent with DFT-calculation results for a model compound. Compounds  $\mathbf{1}_{14}$ -FSI and  $\mathbf{1}_{14}$ -TFSI form thermotropic  $Ia\bar{3}d$ -type bicontinuous cubic mesophases composed of two interdigitated single-gyroid structures of opposite handedness. We propose that close-packing of molecules  $\mathbf{1}_{14}$ -X stabilizes the different atropisomers due to AIA, which, in turn, promotes the formation of helical structures with different senses. This concept constitutes a new molecular-design principle, not only for developing bicontinuous cubic liquid crystals, but also to obtain functional small molecules and polymers that self-organize into helical supramolecular assemblies.<sup>[24,25]</sup> For instance, the architecture of salts  $\mathbf{1}_n$ -X can be used to design new chiral ionic liquids, which have attracted attention as media for asymmetric organic synthesis and chiral chromatography.<sup>[26]</sup>

## Acknowledgements

This work was supported by the Japan Society for the Promotion of Science, Grant-in-Aid for Scientific Research (B) (no. 17H03038). T.K. is grateful for financial support from the JSPS Research Fellowships for Young Scientists (no. JP 18J21088). We are grateful to Dr. N. Terrill and Dr. O. Shebanova for their help with the SAXS experiments at Beamline I22 of the Diamond Light Source (Oxfordshire, UK). We thank Prof. Keiichi Noguchi at Tokyo University of Agriculture and Technology for his help with the 2D NOESY NMR measurements. The authors acknowledge funding for this work from EPSRC (EP-K034308, EP-P002250). Y.L. thanks CSC for a stipend and the University of Sheffield for waiving its tuition fee. K.G. acknowledges the Institute for Basic Science (IBS-R019-D1) for support. The quantum-chemical calculations were performed at the Research Center for Computational Science, Okazaki, Japan.

## Conflict of interest

The authors declare no conflict of interest.

**Keywords:** atropisomers · bicontinuous cubic phase · double-gyroid structures · liquid crystals · self-organization

- [1] a) X. Zeng, G. Ungar, M. Impéror-Clerc, *Nat. Mater.* **2005**, *4*, 562; b) H.-C. Kim, S.-M. Park, W. D. Hinsberg, *Chem. Rev.* **2010**, *110*, 146; c) L. Wu, W. Zhang, D. Zhang, *Small* **2015**, *11*, 5004.
- [2] a) B.-K. Cho, A. Jain, S. M. Gruner, U. Wiesner, *Science* **2004**, *305*, 1598; b) T. Ichikawa, M. Yoshio, A. Hamasaki, T. Mukai, H. Ohno, T. Kato, *J. Am. Chem. Soc.* **2007**, *129*, 10662.
- [3] a) H. Yu, X. Qiu, S. P. Nunes, K. V. Peinemann, *Nat. Commun.* **2014**, *5*, 4110; b) A. Zabara, R. Negrini, O. Onaca-Fischer, R. Mezzenga, *Small* **2013**, *9*, 3602.
- [4] C.-F. Cheng, H.-Y. Hsueh, C.-H. Lai, C.-J. Pan, B.-J. Hwang, C.-C. Hu, R.-M. Ho, *NPG Asia Mater.* **2015**, *7*, e170.
- [5] a) M. Impéror-Clerc, *Curr. Opin. Colloid Interface Sci.* **2005**, *9*, 370; b) D. W. Bruce, *Acc. Chem. Res.* **2000**, *33*, 831; c) P. Fuchs, C. Tschierske, K. Raith, K. Das, S. Diele, *Angew. Chem. Int. Ed.* **2002**, *41*, 628; *Angew. Chem.* **2002**, *114*, 650; d) S. Kutsumizu, *Isr. J. Chem.* **2012**, *52*, 844.
- [6] a) X. Lu, V. Nguyen, M. Zhou, X. Zeng, J. Jin, B. J. Elliott, D. L. Gin, *Adv. Mater.* **2006**, *18*, 3294; b) M. Henmi, K. Nakatsuji, T. Ichikawa, H. Tomioka, T. Sakamoto, M. Yoshio, T. Kato, *Adv. Mater.* **2012**, *24*, 2238; c) T. Sakamoto, T. Ogawa, H. Nada, K. Nakatsuji, M. Mitani, B. Soberats, K. Kawata, M. Yoshio, H. Tomioka, T. Sasaki, M. Kimura, M. Henmi, T. Kato, *Adv. Sci.* **2018**, *5*, 1700405.
- [7] a) T. Kato, M. Yoshio, T. Ichikawa, B. Soberats, H. Ohno, M. Funahashi, *Nat. Rev. Mater.* **2017**, *2*, 17001; b) T. Ichikawa, T. Kato, H. Ohno, *J. Am. Chem. Soc.* **2012**, *134*, 11354.
- [8] *Handbook of Liquid Crystals*, 2nd ed. (Eds.: J. W. Goodby, P. J. Collings, T. Kato, C. Tschierske, H. Gleeson, P. Raynes, V. Vill), Wiley-VCH, Weinheim, **2014**.
- [9] S. Diele, *Curr. Opin. Colloid Interface Sci.* **2002**, *7*, 333.
- [10] R. Holyst, *Nat. Mater.* **2005**, *4*, 510.
- [11] a) K. Ozawa, Y. Yamamura, S. Yasuzuka, H. Mori, S. Kutsumizu, K. Saito, *J. Phys. Chem. B* **2008**, *112*, 12179; b) S. Kutsumizu, Y. Yamada, T. Sugimoto, N. Yamada, T. Udagawa, Y. Miwa, *Phys. Chem. Chem. Phys.* **2018**, *20*, 7953.
- [12] a) M. Vogrin, N. Vaupotic, M. M. Wojcik, J. Mieczkowski, K. Madrak, D. Pocięcha, E. Gorecka, *Phys. Chem. Chem. Phys.* **2014**, *16*, 16067; b) T. Yamamoto, I. Nishiyama, M. Yoneya, H. Yokoyama, *J. Phys. Chem. B* **2009**, *113*, 11564.
- [13] a) C. Dressel, T. Reppe, M. Prehm, M. Brautzsch, C. Tschierske, *Nat. Chem.* **2014**, *6*, 971; b) C. Dressel, F. Liu, M. Prehm, X. Zeng, G. Ungar, C. Tschierske, *Angew. Chem. Int. Ed.* **2014**, *53*, 13115; *Angew. Chem.* **2014**, *126*, 13331.
- [14] G. Bringmann, A. J. P. Mortimer, P. A. Keller, M. J. Gresser, J. Garner, M. Breuning, *Angew. Chem. Int. Ed.* **2005**, *44*, 5384; *Angew. Chem.* **2005**, *117*, 5518.
- [15] R. Noyori, H. Takaya, *Acc. Chem. Res.* **1990**, *23*, 345.
- [16] Z. Zhao, P. Lu, J. W. Y. Lam, Z. Wang, C. Y. K. Chan, H. H. Y. Sung, I. D. Williams, Y. Mab, B. Z. Tang, *Chem. Sci.* **2011**, *2*, 672.
- [17] a) C. Escolástico, M. D. Santa María, R. M. Claramunt, M. L. Jimeno, I. Alkorta, C. Foces-Foces, F. Hernández Cano, J. Elguero, *Tetrahedron* **1994**, *50*, 12489; b) R. M. Claramunt, C. Escolástico, J. Elguero, *ARKIVOC* **2001**, *1*, 172.
- [18] Since the zones that are designated as I and I' in Figure 2c correspond to the same molecular conformation, the number of stable conformers is in fact three rather than four.

- [19] K. R. Gibson, L. Hitzel, R. J. Mortishire-Smith, U. Gerhard, R. A. Jelly, A. J. Reeve, M. Rowley, A. Nadin, A. P. Owens, *J. Org. Chem.* **2002**, *67*, 9354.
- [20] M. Zanatta, J. Dupont, G. N. Wentz, F. P. dos Santos, *Phys. Chem. Chem. Phys.* **2018**, *20*, 11608.
- [21] a) V. Castelletto, I. W. Hamley, *Curr. Opin. Solid State Mater. Sci.* **2004**, *8*, 426; b) G. S. Doerk, K. G. Yager, *Mol. Syst. Des. Eng.* **2017**, *2*, 518.
- [22] a) A. Mathis, M. Galin, J. C. Galin, B. Heinrich, C. G. Bazuin, *Liq. Cryst.* **1999**, *26*, 973; b) F. Neve, M. Impéror-Clerc, *Liq. Cryst.* **2004**, *31*, 907; c) P. Massiot, M. Impéror-Clerc, M. Veber, R. Deschenaux, *Chem. Mater.* **2005**, *17*, 1946; d) A. J. Boydston, C. S. Pecinovsky, S. T. Chao, C. W. Bielawski, *J. Am. Chem. Soc.* **2007**, *129*, 14550; e) W. Dobbs, B. Heinrich, C. Bourgeois, B. Donnio, E. Terazzi, M.-E. Bonnet, F. Stock, P. Erbacher, A.-L. Bolcato-Bellemin, L. Douce, *J. Am. Chem. Soc.* **2009**, *131*, 13338; f) M. A. Alam, J. Motoyanagi, Y. Yamamoto, T. Fukushima, J. Kim, K. Kato, M. Takata, A. Saeki, S. Seki, S. Tagawa, T. Aida, *J. Am. Chem. Soc.* **2009**, *131*, 17722; g) G. P. Sorenson, K. L. Coppage, M. K. Mahanthappa, *J. Am. Chem. Soc.* **2011**, *133*, 14928; h) T. Ichikawa, M. Yoshio, A. Hamasaki, S. Taguchi, F. Liu, X. Zeng, G. Ungar, H. Ohno, T. Kato, *J. Am. Chem. Soc.* **2012**, *134*, 2634; i) B. Soberats, M. Yoshio, T. Ichikawa, S. Taguchi, H. Ohno, T. Kato, *J. Am. Chem. Soc.* **2013**, *135*, 15286; j) G. Park, K. Goossens, T. J. Shin, C. W. Bielawski, *Chem. Eur. J.* **2018**, *24*, 6399; k) T. Kobayashi, Y. Li, A. Ono, X. Zeng, T. Ichikawa, *Chem. Sci.* **2019**, *10*, 6245.
- [23] a) K. Goossens, K. Lava, C. W. Bielawski, K. Binnemans, *Chem. Rev.* **2016**, *116*, 4643; b) K. V. Axenov, S. Laschat, *Materials* **2011**, *4*, 206; c) K. Binnemans, *Chem. Rev.* **2005**, *105*, 4148.
- [24] a) D. J. Hill, M. J. Mio, R. B. Prince, T. S. Hughes, J. S. Moore, *Chem. Rev.* **2001**, *101*, 3893; b) T. Nakano, Y. Okamoto, *Chem. Rev.* **2001**, *101*, 4013; c) E. Yashima, K. Maeda, H. Iida, Y. Furusho, K. Nagai, *Chem. Rev.* **2009**, *109*, 6102; d) Y.-Z. Ke, Y. Nagata, T. Yamada, M. Sugimoto, *Angew. Chem. Int. Ed.* **2015**, *54*, 9333; *Angew. Chem.* **2015**, *127*, 9465.
- [25] a) S. T. Trzaska, H.-F. Hsu, T. M. Swager, *J. Am. Chem. Soc.* **1999**, *121*, 4518; b) T. Kato, T. Matsuoka, M. Nishii, Y. Kamikawa, K. Kanie, T. Nishimura, E. Yashima, S. Ujiié, *Angew. Chem. Int. Ed.* **2004**, *43*, 1969; *Angew. Chem.* **2004**, *116*, 2003; c) J. Barberá, L. Puig, P. Romero, J. L. Serrano, T. Sierra, *J. Am. Chem. Soc.* **2005**, *127*, 458; d) G. Shanker, M. Prehm, C. V. Yelamaggad, C. Tschierske, *J. Mater. Chem.* **2011**, *21*, 5307; e) J. Hu, T. Zhu, C. He, Y. Zhang, Q. Zhang, G. Zou, *J. Mater. Chem. C* **2017**, *5*, 5135; f) T. Wöhrle, I. Wurzbach, J. Kirres, A. Kostidou, N. Kapernaum, J. Litterscheidt, J. C. Haenle, P. Staffeld, A. Baro, F. Giesselmann, S. Laschat, *Chem. Rev.* **2016**, *116*, 1139.
- [26] a) T. Payagala, D. W. Armstrong, *Chirality* **2012**, *24*, 17; b) P. Wasserscheid, A. Bösmann, C. Bolm, *Chem. Commun.* **2002**, 200; c) Z. Wang, Q. Wang, Y. Zhang, W. Bao, *Tetrahedron Lett.* **2005**, *46*, 4657.

Manuscript received: January 9, 2020

Revised manuscript received: February 17, 2020

Accepted manuscript online: March 4, 2020

Version of record online: March 17, 2020